International Journal of Concrete Structures and Materials
Vol. 2, No. 1, pp. 57~62, June 2008

Ultimate Strength of Concrete Barrier by the Yield Line Theory

Se-Jin Jeon,[1)] Myoung-Sung Choi,[2)] and Young-Jin Kim[2)]

(Received October 26, 2007, Revised March 26, 2008, Accepted April 7, 2008)

Abstract: When the yield line theory is used to estimate the ultimate strength of a concrete barrier, it is of primary importance that the correct assumption is made for the failure mode of the barrier. In this study, a static test was performed on two full-scale concrete barrier specimens of Korean standard shape that simulate the actual behavior of a longitudinally continuous barrier. This was conducted in order to verify the failure mode presented in the AASHTO LRFD specification. The resulting shape of the yield lines differed from that presented in AASHTO when subjected to an equivalent crash load. Furthermore, the ultimate strengths of the specimens were lower than the theoretical prediction. The main causes of these differences can be attributed to the characteristics of the barrier shape and to a number of limitations associated with the classical yield line theory. Therefore, a revised failure mode with corresponding prediction equations of the strength were proposed based on the yield lines observed in the test. As a result, a strength that was more comparable to that of the test could be obtained. The proposed procedure can be used to establish more realistic test levels for barriers that have a similar shape.

Keywords: concrete barrier, yield line theory, ultimate strength, crack, static test.

1. Introduction

A barrier should be able to perform a variety of functions, such as preventing a vehicle from running off the road and minimizing occupant injury and vehicle wreckage. Rigid concrete barriers have been widely used on bridges constructions, on overpasses and on general roads, since they show superior performance over deformable metal barriers in several points. Due to the minimized displacement of the barrier, a rigid concrete barrier is able to prevent a vehicle from running off the road, leading it back to the normal road traffic.

While there are a number of Korean provisions[1,2] that are referred to in the design and safety assessment of barriers, they do not provide any procedure by which the ultimate strength of a concrete barrier can be predicted. Conversely, among foreign provisions, the AASHTO LRFD (Load and Resistance Factor Design) specification[3] provides detailed formulas that can be used to calculate the ultimate strength according to the yield line theory. These formulas have also been adopted in Korea to determine the corresponding test level for a specific barrier.[4] According to one Korean provision,[2] the performance of the barrier is classified into seven test levels based on impact severity. In addition, there are a number of standard concrete barrier shapes that are recommended by the Korea Highway Corporation. Consequently, a reasonable evaluation of the ultimate strength or load-resisting capacity of the barrier is a crucial factor for determining the actual test level corresponding to that barrier. Although the most reliable and authentic way to verify the ultimate capacity of the barrier may be to carry out a vehicle crash test,[2,5] such a test requires a specially-designed, large-scale test field and facilities, and is an extremely expensive procedure. Consequently, the vehicle crash test is often regarded only as a tool for final verification. The theoretical approach is one of a number of methodologies used to evaluate the ultimate strength of a barrier, such as the static test, computer simulation, the pendulum test and theoretical assessment. Due to its versatility and convenience, the theoretical approach, obtained through various formulas, is of considerable importance, especially at the design stage or for the preliminary safety assessment of a new type of barrier.

The yield line theory and related formulas for the concrete barrier were originally proposed by Hirsch[6] and are presented in AASHTO LRFD, as shown in Fig. 1 and in Eqs. (1) and (2). The equations can be derived by considering an equality between the external and internal works, and by manipulating the partial differentiation that accompanies the upper bound theorem.[7]

$$L_c = \frac{L_t}{2} + \sqrt{\left(\frac{L_t}{2}\right)^2 + \frac{8H(M_b + M_w)}{M_c}} \tag{1}$$

$$R_w = \left(\frac{2}{2L_c - L_t}\right)\left(8M_b + 8M_w + \frac{M_c L_c^2}{H}\right) \tag{2}$$

where, H: height of barrier, L_c: critical length of yield line, L_t: longitudinal length of distribution of impact force (F_t), R_w: resistance or ultimate strength of the barrier, M_b: flexural resistance of

[1)]KCI member, Daewoo Institute of Construction Technology, Suwon 440-210, Korea. *E-mail: jsj@dwconst.co.kr*
[2)]KCI member, Daewoo Institute of Construction Technology, Suwon 440-210, Korea.

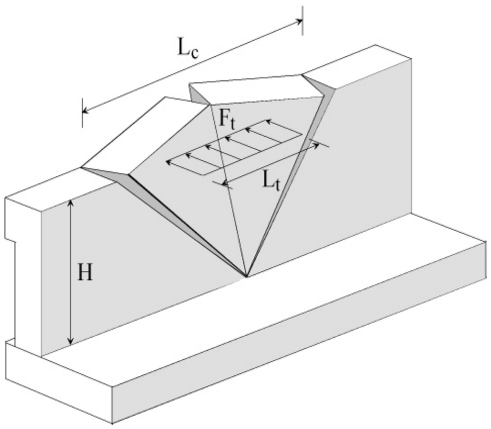

Fig. 1 Yield line theory for a concrete barrier.

the beam at the top of the barrier, M_c : flexural resistance per unit length of the barrier about its longitudinal axis, and M_w : flexural resistance of the barrier about its vertical axis.

However, in recent experimental studies[8-10] conducted in Korea on the failure modes of domestic barriers, it has been shown that the yield lines differ somewhat from the original shape presented in AASHTO LRFD, and depicted in Fig. 1. Static tests were therefore performed in this study to provide further verification of the failure mode and yield line theory presented in AASHTO. To this aim, two full-scale concrete barrier specimens were manufactured, which have the standard shape used throughout Korea. Based on the test results, a number of alternative yield lines were compared that more closely match the actual failure mode than the original theory. Prediction equations for the ultimate strength corresponding to each shape of the yield line were also proposed, and were compared with the measured values, in order to select the best-fit equation. Also, the effects of longitudinal discontinuity on the failure mode and ultimate strength of the barrier were discussed in detail.

2. Effect of longitudinal discontinuity

In Fig. 1, it is assumed that the barrier is monolithically constructed in a longitudinal direction. This results in the yield line shown in Fig. 1 as a consequence of two-way flexural behavior. However, there are some barriers that have longitudinal discontinuity, such as at the expansion joint and at the joint of the precast concrete barriers without any joint-connecting system between the barrier segments. In these cases, it is possible for a vehicle to crash near a point of discontinuity, which would result in a different failure mode from that of the usual shape shown in Fig. 1. In AASHTO LRFD, this is treated as a special case, where a modified version of Eqs. (1) and (2) is provided. Another possibility also arises in the case where failure of the barrier is caused not by typical two-way flexural action, but by one-way cantilevered flexure, depending on the longitudinal length (L) of the longitudinally continuous part of the barrier. While it is specified in AASHTO that the cantilevered failure mode should also be checked, a detailed procedure is not presented. In this study, a more systematic approach will be made in terms of the discontinuity.

While the vehicle crash load specified in AASHTO is approximated by an equivalent line load, it is tentatively regarded as a point load in this discussion in order to maintain clarity. The discussion can be easily extended to a case of the line load. It is assumed that the load is applied to the top of the barrier, since this would present the most adverse case. The bottom of the barrier is either supported by a deck on a bridge or by the foundation in a road. In both cases, the bottom of the barrier can be approximated by a fixed support. The failure modes can then be largely divided into four cases, as demonstrated in Fig. 2. Flexural resistances M_c and M_w are similarly introduced, as in Eq. (1).

It is further assumed that M_c is constant over the barrier section. It is generally difficult to obtain an exact flexural resistance along diagonal yield lines, since barrier reinforcements are arranged in vertical and longitudinal directions. An indirect way to overcome this problem is to separate the flexural resistance along the diagonal line into the contribution made by the vertical and longitudinal directions. The ultimate strengths of the barrier for various cases can then be derived using a minimization process by partial differentiation, as follows.

Crash at a joint with diagonal failure (case A of Fig. 2(a)):

$$P = 2\sqrt{\frac{M_c M_w}{H}} \quad with \; L_c = \sqrt{\frac{M_w H}{M_c}} \tag{3}$$

Crash at a general part with diagonal and vertical failure (case A of Fig. 2(b)):

$$P = 4\sqrt{\frac{2M_c M_w}{H}} \quad with \; L_c = 2\sqrt{\frac{2M_w H}{M_c}} \tag{4}$$

Crash at a joint or at a general part with horizontal failure (case B of Fig. 2(a) or (b)):

$$P = \frac{L}{H} M_c \tag{5}$$

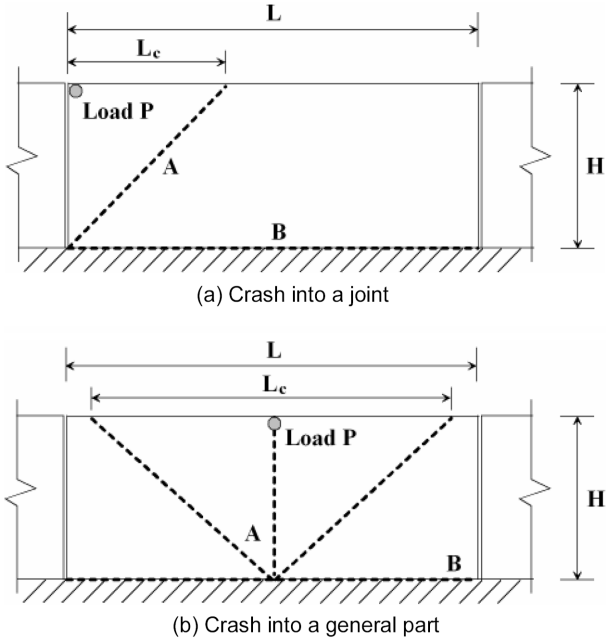

Fig. 2 Failure mode of barrier with joints.

It should be noted that the ultimate strength for the case of horizontal failure depends on an aspect ratio of the continuous part of the barrier. If a vehicle crash can be resisted even by the horizontal or, alternatively, the cantilevered failure mode, it may also be regarded as admissible. However, it should be mentioned that the horizontal failure does not make efficient use of the resistance of the section, since it does not attain the maximum strength achievable with a given section detail. Comparing Eqs. (3) and (5) and assuming $M_c \approx M_w / H$, it can be seen that diagonal failure is ensured when $L > 2H$, which implies the minimum longitudinal length required to avoid undesirable horizontal failure for a crash occurring at the joint. In a similar manner, it can be shown that the condition of $L > 4\sqrt{2}H$ ensures the diagonal failure for a crash occurring at the general part of the barrier. For example, given that $H = 1.32$ m, when $L > 7.47$ m, diagonal failure is generated regardless of the crash point shown in Fig. 2. This information can be useful at a preliminary design stage when a location is to be determined of the expansion joint or longitudinal length of the precast barrier segment without a joint connection. It can also be used to determine a suitable longitudinal length for a test specimen that can simulate a longitudinally continuous barrier. It should also be noted that the crash resistance of the joint is always less than that of the general part of the barrier. It is therefore desirable to minimize the number of joints of discontinuity.

3. Static test of concrete barrier

Two sets of full-scale test specimens were prepared based on the standard barrier shape-2 (Fig. 3) used in Korea, in order to address the theoretical failure mode and ultimate strength by comparing these with the test results. The design compressive strength of the concrete is 35 MPa and the yield strength of the steel is 400 MPa. Sections of the specimen were designed in such a way that the failure would occur at the barrier rather than at the deck, in order to focus on the yield line of the barrier. The equivalent crash load of the vehicle was simulated by a line load (L_t in Fig. 1) with a length of either 1,070 mm or 2,440 mm, corresponding to TL (Test Level)-4 or TL-5, respectively, as specified in AASHTO LRFD.[3] An equivalent crash load that can be referred to in a static test of the barrier is not presented in Korean provisions.

A longitudinal length of 6 m for the specimen was determined by preliminary analyses, so that it could simulate the actual behavior of the longitudinally continuous barrier. The transverse displacements were restrained at both ends of the specimen, which was longitudinally cut with this length. A computer-based analysis[11] (refer to Fig. 4) was then carried out and the results showed that displacements and stress distribution of the specimen are similar to those of the actual continuous barrier. It was also verified that the length is sufficient to generate the yield line shown in Fig. 1. In terms of the yield line, the length of the specimen should be longer than L_c and should be long enough to prevent a cantilevered failure mode B, as shown in Fig. 2(b). Alternatively, if suitable restraints are applied to the cutting edges of the specimen, as they are in this test, then the cantilevered mode can also be prevented, even when the specimen has a shorter length than that expected in the unrestrained condition. An actuator was used to load the specimen up to the point of failure of the barrier (Fig. 5). References 12 and 13 provide further details on the static test.

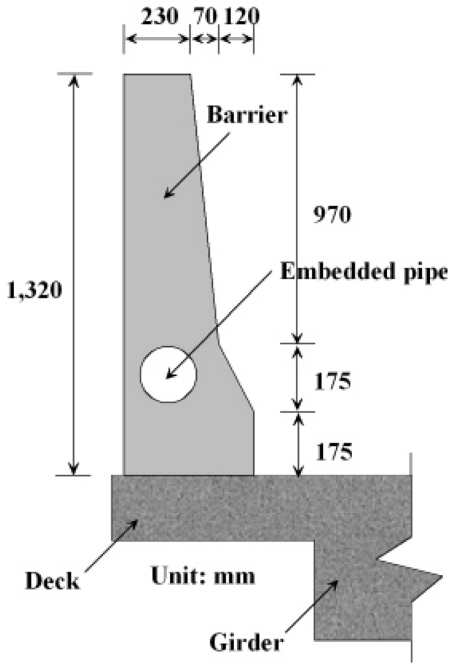

Fig. 3 Section of a test specimen.

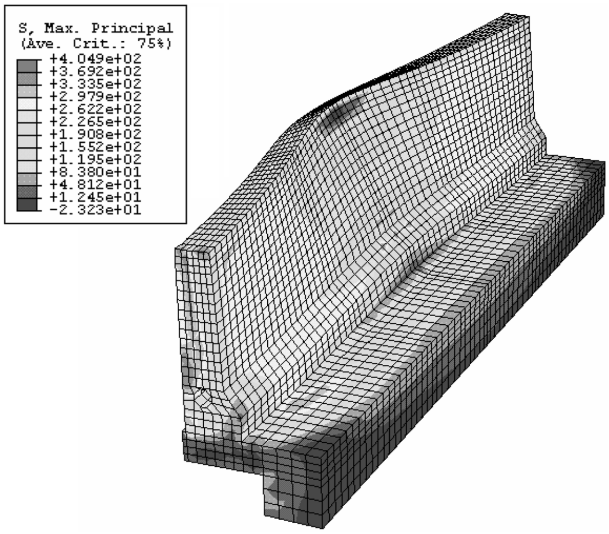

Fig. 4 Finite element analysis for a test specimen.

Fig. 6 shows the cracking pattern that occurs on the front face of each specimen according to the load increment.

4. Yield line and ultimate strength of the barrier

By observing the cracking pattern of the two barriers shown in Fig. 6, it can be seen that the yield lines somewhat differ from those specified in AASHTO LRFD (Fig. 1). Firstly, the cracks mainly occur from above the upper folded line (point A in Fig. 6), rather than from the lower end of the barrier, as illustrated in AASHTO. This may be attributed to a characteristic of the barrier shape, where it becomes narrower from the lower end to the upper end, creating two folded lines. Moreover, the number of main reinforcements provided in the upper side of point A is about half of that provided in the lower side. As a result, point A plays the

Fig. 5 Static test of concrete barrier.

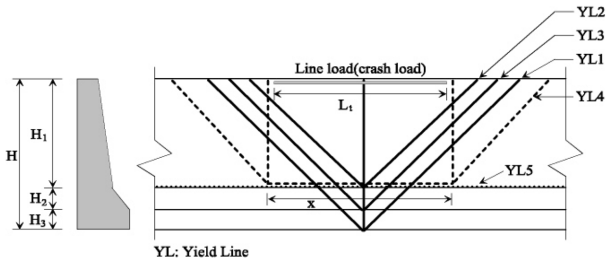

Fig. 7 Alternatives for the barrier yield lines.

role of a continuous semi-fixed support. Secondly, the overall shape of the yield lines did not form that of a triangle, as was shown in Fig. 1, but was rather a trapezoidal form including a horizontal yield line below the loaded area.

Therefore, according to the test results of this study, some revision will need to be made on the conventional yield line theory specified in AASHTO LRFD in order to be able to better predict the ultimate strength of the Korean standard barrier. To this aim, a proposal is made for a revised yield line shape that is more comparable to that of the test results and the prediction equations of the ultimate strength are derived based on this proposed yield line.

Fig. 7 shows several alternative yield lines (failure modes) conceivable for the specimen barriers when subjected to a vehicle crash. Because YL5 cannot be developed in a longitudinally continuous barrier, it is omitted in this discussion. YL1 is the original shape, as presented in AASHTO, and Eqs. (1) and (2) are used to calculate the ultimate strength. While YL2 and YL3 have a similar triangular shape to that of YL1, it is assumed that the yield lines develop above the folded lines of the barrier, taking into account the characteristic of the shape. In these cases, the corresponding ultimate strengths can be readily obtained by replacing H in Eqs. (1) and (2) with H_1 for YL2 and $H_1 + H_2$ for YL3. YL3 was previously proposed in reference 8, where a series of tests were carried out for the standard barrier shape-1 that has a lower height than that of shape-2 used in this study. The longitudinal length and restraint conditions of the specimen also differed from those of the specimen used in this study. When only the yield lines with a triangular shape are considered, YL2 has more similarity with the present test results than either YL1 or YL3. However, further observation of the yield line shown in Fig. 6 reveals that the actual yield line cannot be depicted in the triangular shape. Therefore, YL4, a revised yield line, is proposed in this study, which has more similarity with the test results than any of the other yield lines. It should be noted that YL4 can also be regarded as a geometrically possible failure mechanism.

Fig. 8 shows a detailed geometrical description for a derivation of the equations that are relevant to YL4, where $x \geq L_t$. The two variables of x and α should be considered during the derivation in order to explicitly determine the trapezoidal shape, while one variable is enough to determine the triangular yield line.

The external work W performed by a line load w_t with a result-

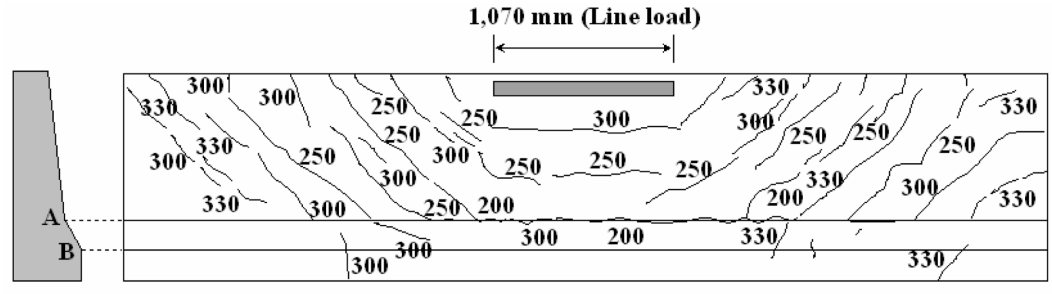

(a) Specimen 1

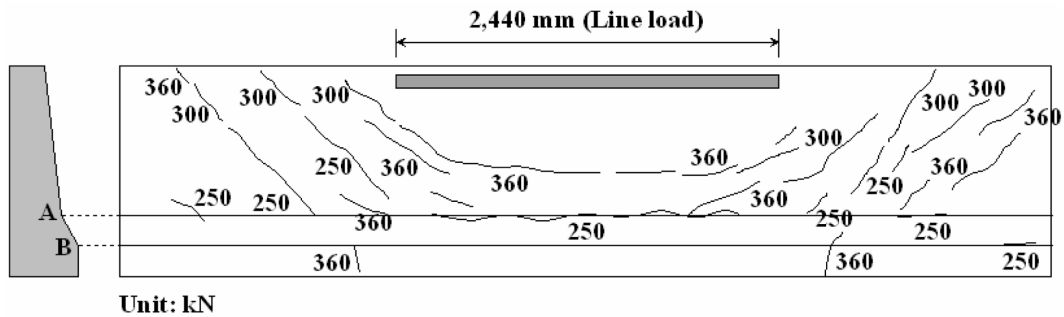

(b) Specimen 2

Fig. 6 Cracking pattern of barrier.

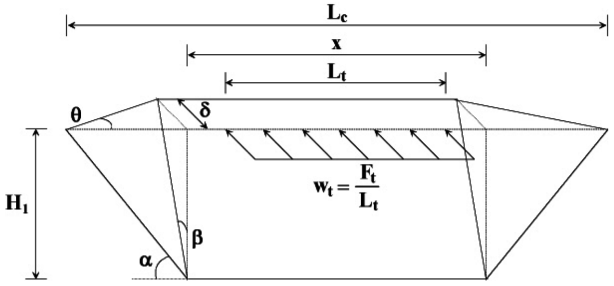

Fig. 8 Detailed failure mode for YL4.

ant force F_t can be written as Eq. (6).

$$W = w_t \delta L_t = \frac{F_t}{L_t} \cdot \frac{\theta H_1}{\tan\alpha} \cdot L_t = \frac{F_t \theta H_1}{\tan\alpha} \quad (6)$$

The internal work U performed by M_{w1} and M_{c1} can be derived as in Eq. (7), where the notations of M_{w1} and M_{c1} are the same as those for Eq. (2), but the additional subscript 1 is introduced in order to indicate the moments within the height H_1.

$$U = U_w + U_c = 4M_{w1}\theta + M_{c1}(2H_1/\tan\alpha + x)\beta \quad (7)$$

When an equality is considered between the external and internal works and they are rearranged with a relationship between θ and β, Eq. (8) is obtained.

$$F_t = \frac{4M_{w1}\tan\alpha}{H_1} + \frac{2M_{c1}}{\tan\alpha} + \frac{M_{c1}x}{H_1} \quad (8)$$

Minimizing Eq. (8) with respect to both x and α, according to the upper bound theorem of the yield line theory, $\tan\alpha = \sqrt{M_{c1}H_1/2M_{w1}}$ and $x = L_t$ are obtained. Placing these variables into Eq. (8), the ultimate strength R_w (Eq. (9)) can finally be obtained.

$$R_w = 4\sqrt{\frac{2M_{c1}M_{w1}}{H_1}} + \frac{M_{c1}L_t}{H_1} \quad (9)$$

Taking into account $x < L_t$, the relevant equations and the minimization process become more complex. However, it should be mentioned that the calculated ultimate strength, using this method, is between that of YL2 and YL4, and that YL4 produces less ultimate strength than that of YL2 in this study, as shown in Table 1. Consequently, the case of $x < L_t$, which is a general case of YL2, does not need to be considered as a candidate to produce a minimum strength.

In Table 1, a comparison is made of the ultimate strengths evaluated from each yield line. Among these, the strength of YL4 is more similar to that of the test result in both specimens. This is expected, because the shape of YL4 is more similar to that of the failure mode of the test and it provides the minimum value. Considering the upper bound theorem of the yield line theory, it is plausible that the yield line that provides the minimum strength is most likely to occur. When, for simplicity, the candidates are limited to the triangular yield line, the strength of YL2 shows more similarity to the test results than that of other yield lines, as was expected based on the similarity of the failure modes.

However, some difference of the values still remains between the test result and the revised theories. This may be attributed to the following causes. Firstly, the cracks were distributed in such a way that it is difficult to determine a typical shape for the yield line and for L_c (Fig. 1). There may be an alternative yield line that provides a smaller strength than those already considered. Secondly, in the derivation, a general assumption was made that flexural resistances should not vary significantly along the height of the barrier. However, there are some differences between the resistances along the height, mainly due to the tapered section, and these differences are often averaged. Thirdly, separating the flexural resistance along a diagonal yield line into the resistances about two orthogonal directions is a convenient yet simplified way to derive relevant equations. Finally, it seems that the yield lines were not fully developed even in the ultimate state, since concrete crushing was not observed on the opposite face of the crack. This may result in a lower flexural resistance along the yield line than expected, from the strength design method in flexure. As expected, the theoretical flexural resistances along the yield line are derived on the basis of the concrete crushing in compression and the yielding of the main reinforcements as well as the concrete cracking in tension.

5. Conclusions

A full-scale static test was performed with standard concrete barriers by applying different loading patterns that simulate a vehicle crash. The main purpose of the test was to verify the failure mode and prediction equations of the ultimate strength in terms of the yield line theory presented in the AASHTO LRFD specification. The resulting shapes of the yield lines differed from those presented in AASHTO and the ultimate strengths were lower than the theoretical prediction provided by AASHTO. These differences can mainly be attributed to the specific characteristics of the barrier shape that is being considered. Therefore, a revised failure mode and corresponding prediction equations of the strength based on the actual yield lines were proposed, where several yield line candidates were compared. As a result, a more comparable strength with that of the test could be obtained. Also, the effects of the longitudinal discontinuity on the ultimate strength of the bar-

Table 1 Comparison of ultimate strengths.

Specimen number	L_t (mm)	L_c (mm)					R_w (kN)				
		Analysis				Test	Analysis				Test
		YL1	YL2	YL3	YL4		YL1	YL2	YL3	YL4	
1	1,070	3,845	3,213	3,183	3,697	Not clear	614.0	442.6	513.6	434.3	330.0
2	2,440	4,707	4,114	4,086	5,067	Not clear	751.7	566.2	659.4	528.4	360.0

rier were discussed in detail. It was found that a possibility of the cantilevered failure mode should also be examined by accounting for a continuous longitudinal barrier length. The proposed procedure can be used to establish more realistic test levels for barriers that have similar shapes.

References

1. Korea Road and Transportation Association, *Highway Bridge Design Code*, KRTA, 2005.

2. Ministry of Construction and Traffic, *Guideline for Installation and Management of Road Safety Facilities*, MOCT, 2001.

3. American Association of State Highway and Transportation Officials, *AASHTO LRFD Bridge Design Specifications*, 4th Ed., AASHTO, 2007.

4. Korea Highway Corporation, *Review of Design Methods of the Concrete Barrier on the Bridge*, Korea Highway Corporation, 2002.

5. Ross, H. E., Jr., Sicking, D. L., Zimmer, R. A., and Michie, J. D., *Recommended Procedures for the Safety Performance Evaluation of Highway Features*, National Cooperative Highway Research Program (NCHRP) Report 350, Transportation Research Board & National Research Council, 1993.

6. Hirsch, T. J., *Analytical Evaluation of Texas Bridge Rails to Contain Buses and Trucks*, Research Report 20-2, Texas Transportation Institute, Texas A&M University, 1978.

7. Nielsen, M. P., *Limit Analysis and Concrete Plasticity*, 2nd Ed., CRC Press, 1999.

8. Korea Highway Corporation, *A Study on the Design and the Performance Improvement of Cantilever Part in Bridge Deck with Concrete Rigid Barrier*, Korea Highway Corporation, 2004.

9. Woo, K. S., Kim, J. I., Ra, J. S., and Ahn, S. S., "Dynamic Impact Load and Performance Evaluation of Concrete Rigid Barriers," *Journal of the Korean Society of Civil Engineers*, Vol. 24, No. 5A, 2004, pp. 1053~1063.

10. Kang, J. W., Lee, J. H., Woo, K. S., Ahn, S. S., and Lee, I. G., "A Static Test of Concrete Barrier on Bridge Deck," *Proceedings of the Korea Concrete Institute*, Vol. 16, No. 2, 2004, pp. 33~36.

11. *ABAQUS/Standard 6.3-User's Manual*, Hibbitt, Karlsson & Sorensen, Inc., 2002.

12. Jeon, S. J., Choi, M. S., Kim, Y. J., and Hyun, B. H., "Static Test of Precast Concrete Barrier I. Ultimate Behavior and Test Level," *Journal of the Korean Society of Civil Engineers*, Vol. 27, No. 6A, 2007, pp. 891~899.

13. Jeon, S. J., Choi, M. S., and Kim, Y. J., "Static Test of Precast Concrete Barrier II. Analysis of the Measured Data," *Journal of the Korean Society of Civil Engineers*, Vol. 27, No. 6A, 2007, pp. 901~908.